

Full Paper

Electrochemical Detection of Catechol using Synthesized Titanium Oxide Nanoparticles

Adigerhalli G. Bindu,¹ Ramesh S. Bhat,^{1,*} Shivani,¹ and Ampar C. Hegde²

¹*Department of Chemistry, NMAM Institute of Technology, NITTE (Deemed to be University), Nitte-574110, India*

²*Electrochemistry Laboratory, Department of Chemistry, National Institute of Technology Karnataka, Srinivasnagar, 575025, India*

*Corresponding Author, Tel.: +91 8861037310

E-Mail: rameshbhat@nitte.edu.in

Received: 24 December 2024 / Received in revised form: 26 March 2025 /

Accepted: 27 March 2025 / Published online: 31 March 2025

Abstract- The fabrication of advanced electrodes has garnered significant attention due to their exceptional sensitivity and selectivity for detecting catechol samples. Titanium dioxide nanoparticles (TiO₂ NPs) have emerged as highly effective modifiers for carbon paste electrodes (CPEs), attributed to their unique electrochemical characteristics and enhanced conductivity. In this study, TiO₂ NPs are prepared via the combustion method (CM), offering a reliable strategy for boosting electrode performance. This work aims to synthesize the TiO₂ NPs by using Titanium (III) sulfate as precursor materials, and citric acid as fuel to get the desired TiO₂ NPs. The confirmation of NPs is done through various techniques such as field emission scanning microscopy (FESEM), microstructure analysis by XRD, elemental composition by EDS, and absorption vibration levels by Raman spectroscopy. TiO₂ NPs are used for the development of electrode applications to determine catechol (CC) using carbon paste electrodes (CPE). The electrode surface is modified into a TiO₂ composite carbon paste electrode (TiCCPE). The electrochemical techniques are performed using a phosphate buffer solution (BS) of 0.1 M at a pH range of 7.0 of a two-electron transfer system with scan rates variation from 0.50-0.400 V/s signifies reaction of absorption-controlled process, and concentration studies from 0.2 μM to 1.6 μM with detection and quantification limit of 0.21 μM and 0.71 μM and was found using Linear sweep voltammetry technique (LSV). The electrode modification associated with synthesized TiO₂ NPs assists in an outstanding way to sense the CC, as good sensitivity, stability, selectivity, and reproducibility of catechol detection were assessed using electrochemical techniques throughout the studies.

Keywords- TiO₂ NPs; XRD; Linear sweep voltammetry; Catechol; Modified electrode; Detection limit

1. INTRODUCTION

The trend of chemistry today refers to nanotechnology, as it contains vast applications and particles that can be prepared through various methods like processes under top-down and bottom-up approaches. The prepared nanoparticles are further used to detect the sensitivity and selectivity of biomolecules [1]. Titanium is a good semiconductor with significant interest and applications in the field of electrochemistry. Its properties like morphology, physical and chemical, stability, non-toxicity that help in the ease of further study [2]. Material with applications in a wide range of various fields in pigments, stability of electrode dimension, photocatalysts, optical applications, solar cells, coating, biomedical, sensors, etc. [3].

Pyrocatechol is also popularly known as catechol of phenolic compounds as it is present in plants like tea and vegetables. It shows antioxidation and antiviral effects affecting some enzymes [4]. Even low concentrations are dangerous to humans and animals to degrade and cause environmental pollution [5]. Toxicity leads to central nervous system damage, kidney damage, and also cancerous alterations [6]. They are present in streams in the dye, plastic, resin, plasticizers, paper, cosmetics, etc. Many nations communities suggested and proved that phenols are the number 1 pollutant to the European and Environmental Protection Agency and committee [7]. Widely used in industry as we can observe there are only a few methods to determine catechol by some different modified electrode processing methods such as clay modified, multiwalled, iodine coated, bare indium tin oxide, glassy carbon, electrochemiluminescence, fluorescence, chromatography, pH-related flow injection analysis, spectrometry etc. [8]. The combustion method is considered as the best method for the synthesis of metal oxide NPs, which undergoes combustion of chemicals phase takes place followed by vaporization for the formation of novel properties involved in good compound formation [9]. The carbon material containing products like pores, nanotubes, nanoparticles, graphite as well as graphene serve as a promising, outstanding output for electrochemical analysis as they offer less background current and rapid output, promising redox behaviour, and are cost-effective with easy handling [10].

Linear Sweep Voltammetry is a strong analytical technique that gives evidence for the process of electrochemical output of an analyte. CPE plays an important character due to its low background current is low, cost efficiency, and a well-known method for low concentration findings [11]. The LSV techniques depend on the morphology of the surface and catalytic behaviour of BCPE (Bare carbon paste electrode) and MCPE (modified carbon paste electrode) [12].

This work includes the preparation of TiO₂ NPs through the combustion method and confirmation through FESEM, EDX, XRD, and Raman spectroscopy. Additionally, these TiO₂ NPs further used in the modification of electrodes as TiCCPE. This modification towards electrochemical techniques of LSV, CV, and EIS studies in the pH range, variation of scan rate

and concentration variation with cost-effective, excellent stability, selectivity, sensitivity, and reproducibility in the analysis of CC.

2. EXPERIMENTAL SECTION

2.1. Apparatus and chemicals

Titanium (III) sulphate and citric acid (Sigma Aldrich, India). Electrochemical techniques measurements were performed with the help of a CH instrument linked with a three-electrode system arrangement. Catechol (CC) (moly chem, India), graphite powder, silicon oil, monosodium hydrogen phosphate, and disodium hydrogen phosphate (Hi-media Chemicals), All the chemicals utilized are of investigative standard grade and worked on them without refinement. Phosphate buffer solution (BS) was prepared by intermixing monosodium hydrogen phosphate and disodium hydrogen phosphate in a proper volume and carried out at room temperature. All the FESEM, XRD, EDX, and Raman spectroscopy were analysed and reported from the Central Research Facility, NITK, Mangalore. SEM from Vijnana bhavan Mysore University Mysore.

2.2. Titanium oxide nanoparticles preparation:

Calculated proportional of Titanium (III) sulphate precursor material and citric acid as fuel are thoroughly mixed until a homogenous mixture is formed. The obtained liquid material was poured into a porcelain crucible and heated in a muffle furnace for an hour at 500 °C for the output of powder material. The product was washed in a container several times for the removal of impurities with ethanol and deionised water and dried in a hot air oven for one hour. Through this process sample of titanium oxide nanoparticles was prepared [13].

2.3. Development of fabricated electrode:

The mixture of powder of graphite and silicon oil in a 70:30 proportion and gentle mixing in a mortar leads to the formation of carbon paste. Later, the addition of titanium oxide nanopowder to carbon paste as a composite material. Further, carried out as the Teflon tube cavity material with tightly packed in the analysis of biomolecule sensing throughout the study.

3. RESULTS AND DISCUSSION

3.1. Morphological confirmation of titanium oxide nanoparticles

The morphology of the prepared TiO₂ NPs was analysed by FESEM and was shown in Figure 1. The image shows remarkable changes under the observations through the microscope concerning microstructure, regular arrangement, porosity, particle distribution nature, grain size, and agglomeration of nanoparticles are distinct and well-separated. The absence of

ununiform size clusters suggests reaction involves nucleation and effective production of homogenous NPs. The smooth surface and irregularities indicate the purity along with the quantity of prepared particles. The voids and porous are mainly due to large amounts of gas during combustion. The well clarity in borders of NPs indicates the reproducibility of NPs with having shapes of rhombohedral and smooth surfaces, indicates the purity of NPs with high activity for applications. As the image is of 65000 magnification and in the nano range of 500nm [14].

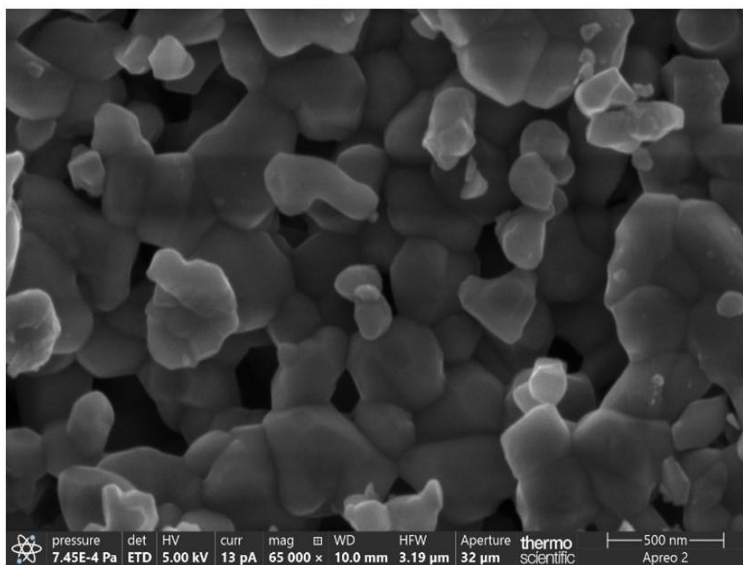


Figure 1. Surface image of the synthesized titanium oxide NPs

The elemental composition of prepared NPs of TiO_2 existence studied with weight % of oxygen (20.4%) and titanium (79.6%) respectively. No other additional peaks present indicate the purity of synthesized NPs was noticed in Figure 2.

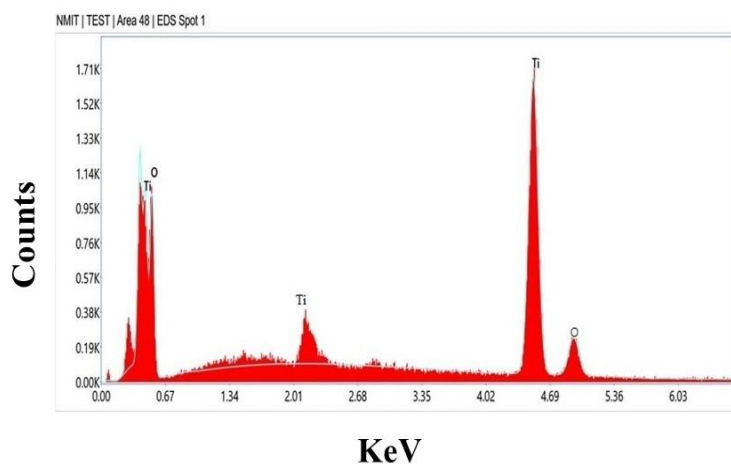


Figure 2. EDX image of synthesized titanium oxide nanoparticles

3.2. Surface analysis by SEM

The surface nature of TiCCPE and BCPE surfaces is displayed in Figure 3(a and b) and analyzed through SEM. Figure 3b reveals a uniform surface with a layer formed by the presence of nanoparticles (NPs), filling voids and creating a smooth texture. This suggests that the electrode surface has been modified and coated with titanium oxide nanoparticles, resulting in a clear and uniform appearance. In contrast, Figure 3a shows a rough, irregular texture with visible surface gaps, indicating higher porosity and less stable electrochemical behavior [15].

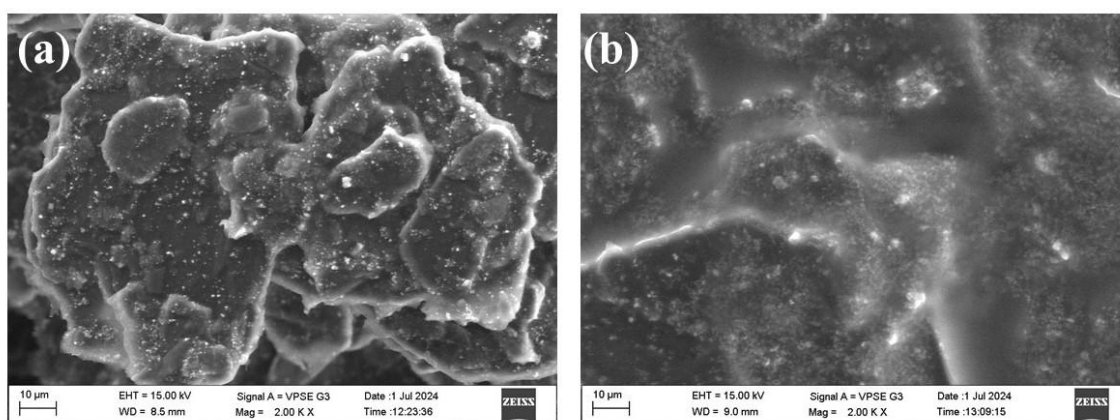


Figure 3. Images of SEM for CPE (a) and TiO₂ CCPE(b)

3.3. XRD analysis

Figure 4 implies the XRD pattern of the synthesized titanium oxide nanoparticles (TiO₂ NPs), with diffraction peaks at 2θ values of 27.72°, 36.35°, 39.5°, 41.45°, 44.3°, 54.54°, 56.95°, 62.89°, and 70.12°, corresponding to the crystallographic planes (110), (103), (200), (112), (210), (105), (221), (204), and (220). These diffraction angles align well with standard values, indicating high crystallinity and purity, as confirmed by JCPDS card number 1-1272. The diffraction patterns confirm the formation of a tetragonal body-centered structure for the TiO₂ NPs. The particle size, calculated using Debye-Scherrer's formula, is approximately 45 nm [16].

3.4. Raman spectrum of prepared TiO₂ NPs

The prepared NPs Raman spectrum is represented in Figure 5. The vibration mode of Eg appears at 144.5 cm⁻¹. Whereas, (A_{1g} + B_{1g}), at 397.7 cm⁻¹, 518 cm⁻¹ confirms B_{1g} and E_g modes, and 641 cm⁻¹ respectively. The stretching modes of the Ti-O peak are associated with E_g at a peak range of 518 cm⁻¹ and 397.7 cm⁻¹. The anatase stretching modes phase of Ti-O and the bending mode of O-Ti-O are respectively. The high crystallinity is identified by its sharp and intense peak nature. The rutile phase absence confirms the synthesized nanoparticles purity.

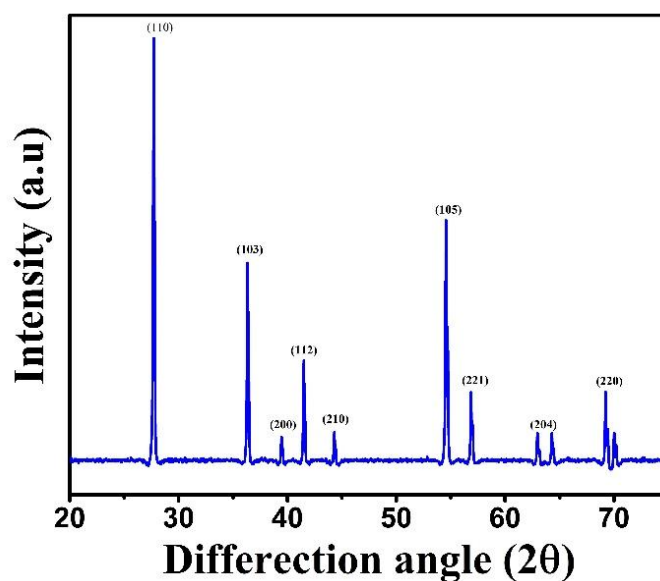


Figure 4. XRD pattern of TiO₂ NPs

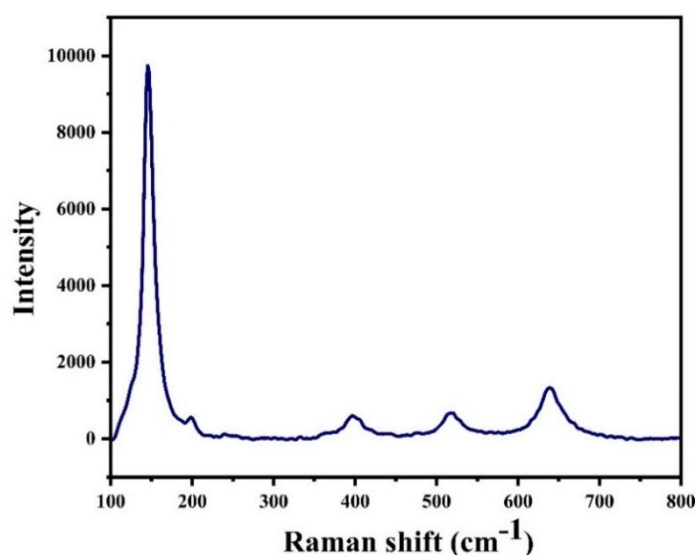


Figure 5. Raman spectroscopy of TiO₂ NPs

3.5. Electrochemical impedance spectroscopy of TiCCPE and CPE surface

EIS signifies the study of the transfer of charge resistance (R_{ct}) and the conductivity of electrode. BS of known concentrations of potassium chloride and potassium ferrocyanide solutions are used for the study. Nyquist plot of both electrodes is shown in Figure 6. The CPE exhibits a larger semicircle (curve a) indicating a lower R_{ct} value. The semicircle size helps identify electron transfer resistance with high conductivity and vice versa. R_{ct} value also corresponds to the diffusion process related to the linear area. By consideration of conductivity and charge transfer resistance of TiCCPE (curve b) is inferior compared to CPE (curve a).

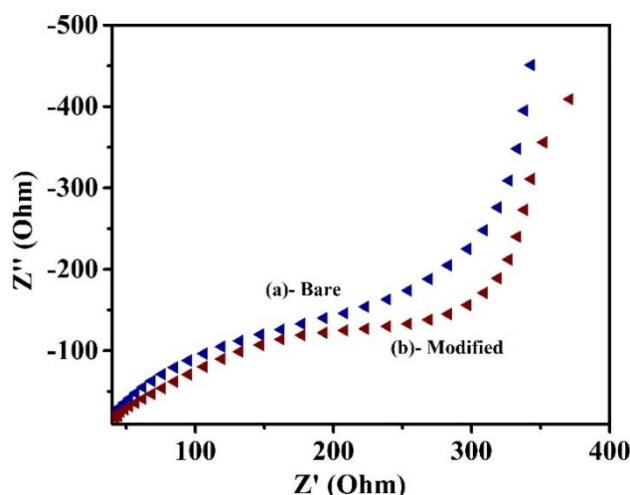


Figure 6. EIS study for CPE (curve a- Bare) and TiCCPE (curve b-Modified)

3.6. Electrochemical redox action on CC at TiCCPE

The LSV of CPE and TiCCPE in BS of 0.2M at pH 7.0 in a 0.6 to -0.4V/s range of potential at a scan rate of 0.1V/s. At the TiCCPE surface. The CC redox peak current increases with a decrease in E_{pa} due to the high active surface area in TiCCPE. This leads to high electron charge transfer between analyte CC and the electrode material. Broad redox peak due to less current intensity in Figure 7a. There was a vigorous reaction of electron transfer taking place in TiCCPE (Figure 7). The electron transfer is due to the conductivity of electrons in the CP of graphite material and an effective surface area region with stability can be absorbed. Indicates current flow and electron transfer easily and quickly in the modified surface of Figure 7b compared to Figure 7a.

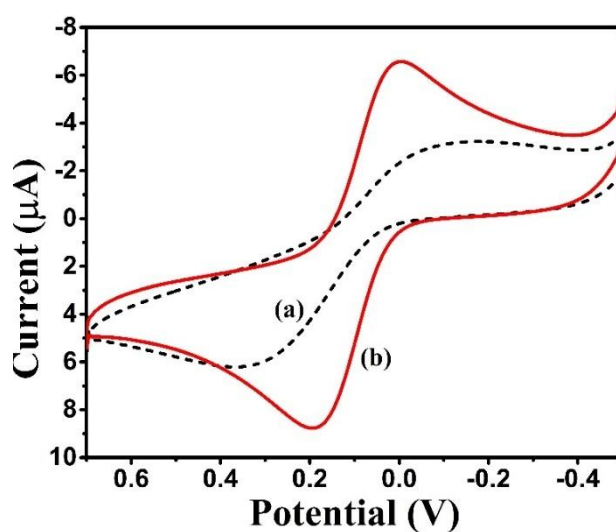


Figure 7. Cyclic voltammogram of BCPE (coloured black) (a) and TiCCPE (coloured red) (b) in 0.2M BS at a pH of 7.0

3.7. Response of CC at various pH

The major response of electrochemical response of bioactive biomolecules is pH. This is the important factor influencing the electrode surface process along with the mechanism, this factor helps in the electrochemical detection of 0.1mM CC in TiCCPE. To analyse the LSV response of analyte compound in different pH ranges of 6.0, 7.0 to 8.0 at TiCCPE (Figure 8). At 0.1M BS, a scan rate of 0.1V/s with a potential range of -0.2V to 1.2V. The noticeable change as an increase in pH, signifies a higher current noticed at 7.0 pH. Where peaks shifted towards the negative pathway indicates higher electrochemical activity towards electrode material. Also, due to the deprotonation of all protons high intense peak current is observed. By the process easily at pH of 6.0 less proton transfer occurs and at pH 7.0 moderate deprotonation occurrence is noticed, which signifies peak current increment also. So, it is considered a suitable pH for sensitivity and selectivity. The Linear regression concentration of E_{pa} and pH is given by equation (1).

$$E_{pa} (V) = -0.1047(-0.0582)(V)(R^2 = 0.9795) \quad (1)$$

The oxidation of CC is pH-dependent on E_{pa} , with slope values equal to 0.059 V/pH of equation (1) is equal to the Nernstian value of theoretical value. The electrochemical oxidation of two numbers of electron and protons transfer system in biosensing of CC using TiCCPE surface of the mechanism shown in Scheme 1. The total protons participated in redox behaviour is calculated using the pH slope value by equation (2).

$$B = \frac{2.303mRT}{nF} \quad (2)$$

Here B signifies the slope value, n is the protons number participating in the redox process of the CC is 2, T remains temperature, R stands for the universal gas constant, and F represents the Faraday law constant.

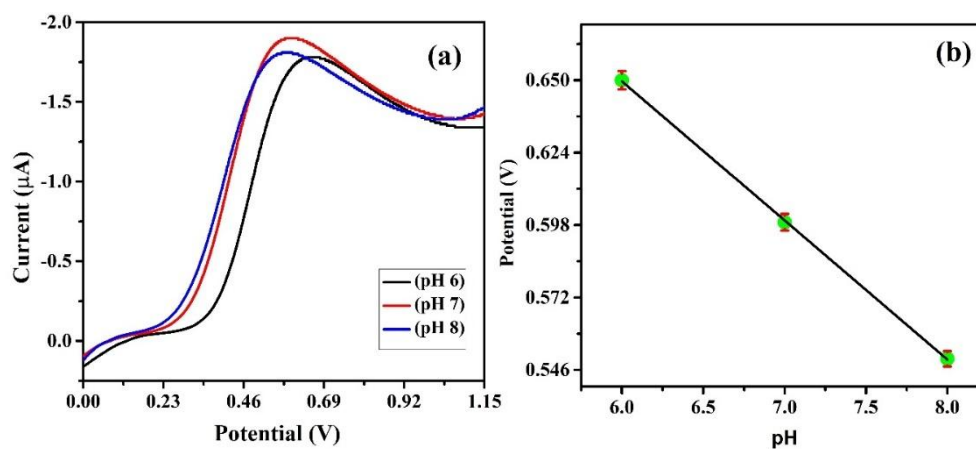
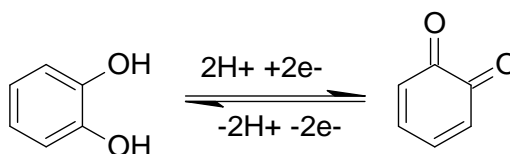


Figure 8. LSV of the TiCCPE in 0.2M BS containing CC with different pH at a scan rate of 0.01V/s. (b) The linearity plot of E_{pa} versus varied pH values



Scheme 1. Redox action of catechol

3.8. Impact on potential sweep rate

The impact on the variation of scan rate (SR) of peak current I_{pa} in 0.1mM CC was studied. Figure 9 at the surface of TiCCPE, LSV of CC at scan rate variations from 0.025V/s to 0.400 V/s for 0.2M BS at a pH range of 7.0 with -0.2V to 1.2 V range of potential at a scan rate of 0.1V/s. Potential versus current in (Figure 9a) and $\log I$ versus $\log (SR)$ show a linear relationship reported in (Figure 9b). The linear regression equation for current in sweep rate is given by equation 3.

$$E_{pa} = -5.2922 + 0.388(R^2 = 0.9917) \quad (3)$$

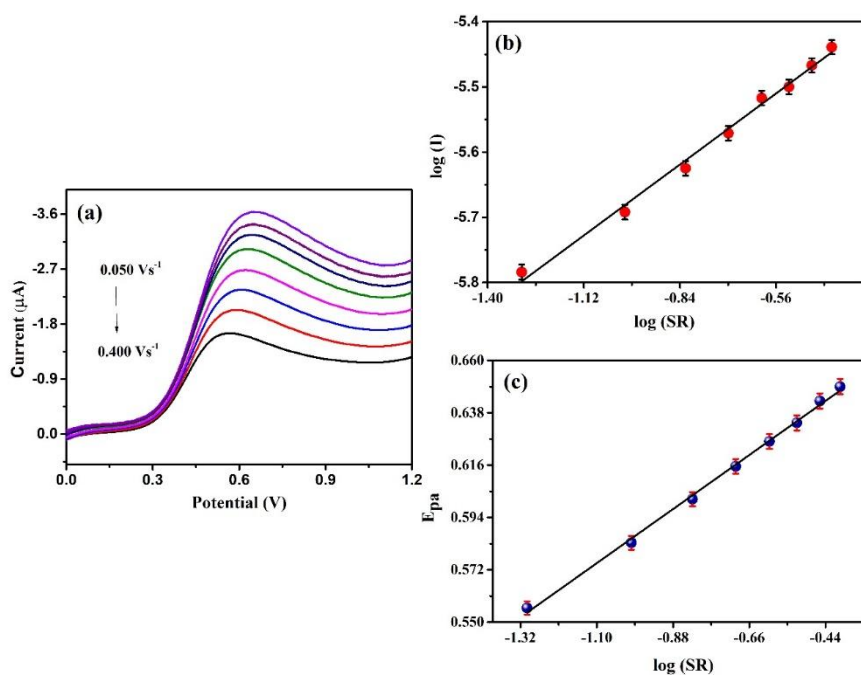


Figure 9. a) Linear sweep voltammetry of CC in 0.2 M BS of 7.0 pH in TiCCPE with SR variation; (b) Graph of the anodic peak of \log current vs. \log SR; (c) Graph of anodic peak potential voltage vs. \log SR

This implies that CC oxidation is at the surface of TiCCPE. The oxidation of the peak moves in the positive direction of potential with an increased SR as the peak current also increases. The linearity of the SR variation demonstrates good selectivity and sensitivity of the detection of CC on the electrode surface. By the observation of the above (equation 3), as the

slope value of $\log(\text{scan rate})$ vs. $\log(\text{current})$, the slope is anywhere near 0.5 and can be easily noticed as diffusion-controlled. Potential versus $\log(\text{SR})$ is noted in (Figure 9c). The slope specifies (Figure 9c) the electrons present in the reaction were found to be 2. The B is the slope value of $\log(\text{SR})$ vs. E_{pa} , T is of absolute temperature, R will be the gas constant, F indicates the Faraday law constant, and N belongs to the number of electrons involved in the reaction 4.

$$B = \frac{2.303RT}{(1-a)nF} \quad (4)$$

3.9. Concentration Variation of CC

The CC electrochemical oxidation was inspected by changing the concentration of analyte 0.1mM CC from 20 μM to 160 μM in 0.2M BS of 7.0 pH with -0.2V to 1.2V potential range at a scan rate of 0.1V/s at TiCCPE as displayed in Figure 10. The plot of current vs. CC concentration describes a fine linear association as concentration increases current also increases with linear regression as in equation 5.

$$I_{pa} = 1.722E - 7 + 4.096(R^2 = 0.9859) \quad (5)$$

The DL and DQ were found to be 0.21 μM and 0.71 μM using DL=3S/BS and QL=10S/BS where DL refers to the detection limit, QL is the quantification limit, S represents the standard deviation of blank and BS indicates the current versus concentration of CC slope. The calculated value displays the electrochemical sensitivity of CC at the micromolar level using the LSV technique. Outcomes explain good selectivity and sensitivity toward CC using the fabricated electrode. Comparison study with another fabricated electrode is listed below in Table 1.

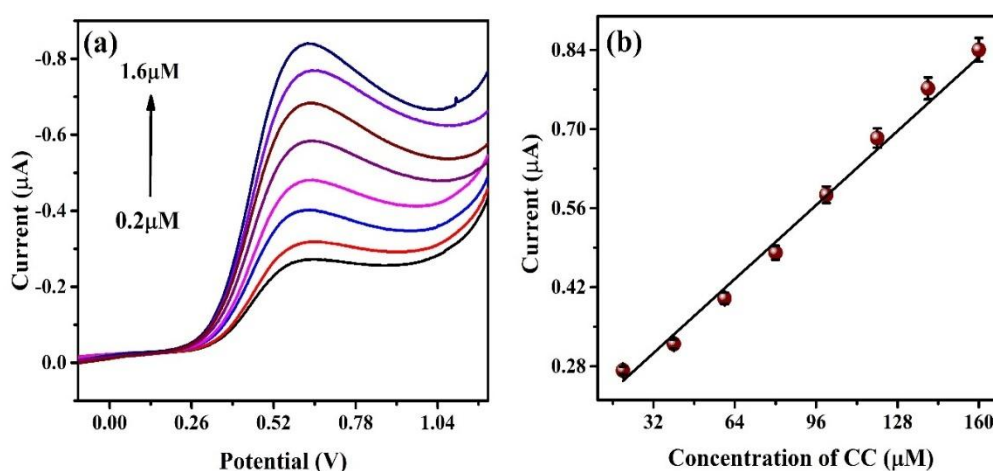


Figure 10. (a) Linear sweep voltammetry of CC with variation in concentrations varying from 0.2 μM to 1.6 μM in BS of 7.0 pH at the TiCCPE surface with 0.1 V/s sweep rate; (b) graph of current (I) vs. concentration (M)

Table1. Comparison study with other fabricated electrodes

Electrode	Linear range	Detection limit	Reference
A-GCE	0.5-200	0.31	[17]
GGR-GCE	0.5-300	0.23	[18]
RGO-NT-GCE	5.5-540	1.8	[19]
Ti-CNT-GCE	1.5-300	0.8	[20]
TiCCPE	0.2-1.6	0.21	Present Work

3.10. Repeatability, stability, and reproducibility of TiCCPE

The reproducibility, stability, and repeatability of the TiCCPE were evaluated by electrochemical analysis of CC in BS 0.2 M of 7.0 pH with 0.1 V/s scan rate using the LSV technique. The TiCCPE reproducibility was examined by fabricating five modified electrodes individually with a constant sample and repeatability was estimated by preparing five different BS samples with a fixed electrode were found of standard deviations of 3.027% and 1.58%, respectively. This analysis suggests that the electrode fabricated is repeatable and reproducible for the analysis of CC. The TiCCPE stability of the fabricated electrode surface was tested by confirming the LSV technique for CC. The stability value was determined by using the noted initial reading before some time and the same detection using the same electrode after some time, the reading of peak current specifies the stability. Here, the calculated value of stability is found to be 96.54%, which offers worthy stability for long-term TiCCPE for the CC analysis.

4. CONCLUSION

In the present work, an eco-friendly, cost-effective, simple, non-risky electrochemical electrode is developed through TiO₂ NPs were synthesized through combustion method using titanium (III) sulfate and citric acid, at 500 °C, their morphological and structural conformation through FESEM as rhombohedral in shape, EDS of oxygen (20.4%) and titanium (79.6%), XRD with crystal size 45 nm and Raman spectroscopy. These NPs were then combined with CP to develop TiCCPE to improve the surface area of MCPE, which shows excellent performance for electrochemical analysis of catechol by enhancing the electron transfer system using Linear sweep voltammetry and electrochemical impedance study. The pH 7.0 is considered optimal pH by variation of pH, and the scan rate variation gives the conclusion of diffusion-controlled reaction with 2 2-electron transfer process. The concentration study gives information about DL and DQ were found to be 0.21 μM and 0.71 μM, with the reproducibility and repeatability of 3.027% and 1.58%, and stability of the modified electrode of 96.54%. The fabricated modified electrode exhibits improved electrochemical behaviour towards the detection of catechol and shows greater sensitivity, selectivity, and reproducibility in the study.

Authors Declarations

- *Declaration of conflict of interest*
The authors confirm that no financial or personal associations influence the research presented in the paper.
- *Ethical Standards Compliance*
The authors state that there are no ethical issues for this type of work.
- *Authorship contribution statement*
Bindu A.G. - Writing the original draft, methodology, and investigation
Ramesh S. Bhat- Supervision, investigation, editing and review, project administration, and validation
Shivani - Writing the original draft, formal analysis, and software analysis
Chitharanjan Hegde - Review and editing
- *Data availability statement*
The data is made available only on request to the corresponding author.

REFERENCES

- [1] M. Mazloun-Ardakani, H. Beitollahi, Z. Taleat, H. Naeimi, and N. Taghavinia, J. Electroanal. Chem. 644 (2010) 1.
- [2] S.R. Kumar, G.P. Mamatha, H.B. Muralidhara, K.Y. Kumar, and M.K. Prashanth, Anal. Bioanal. Electrochem. 7 (2015) 175.
- [3] S.S. Kalanur, J. Seetharamappa, and S.N. Prashanth, Colloids Surf. B Biointerfaces 78 (2010) 217.
- [4] P.A. Kilmartin, and C.F. Hsu, Food Chem. 82 (2003) 501.
- [5] A. Kiani, J.B. Raoof, D. Nematollahi, and R. Ojani, Electroanalysis 17 (2005) 1755.
- [6] K.M. Hassan, A. A. Hathoot, M.F. Abo Oura, and M.A. Azzem, RSC Adv. 8 (2018) 6346.
- [7] S.A. Fathy, F.F. Hamid, A. El Nemr, A. El-Maghraby, E. Serag, Desalination Water Treat. 130 (2018) 98.
- [8] A.B. Teradale, S.D. Lamani, B.E. Kumara Swamy, P.S. Ganesh, and S.N. Das, Adv. Phys. Chem. 1 (2016) 8092860.
- [9] R. Qian, H. Zong, J. Schneider, G. Zhou, T. Zhao, and Y. Li, et al., Catal. Today 335 (2019) 78.
- [10] Y. Zhang, S. Xiao, J. Xie, Z. Yang, P. Pang, and Y. Gao, Sens. Actuators B 204 (2014) 102.
- [11] G. K. Jayaprakash, B. E. Kumara Swamy, S. Rajendrachari, S.C. Sharma, and R. Flores-Moreno, J. Mol. Liq. 334 (2021) 116348.
- [12] J.K.S. Kumara, B.E. Kumara Swamy, G.K. Jayaprakash, S.C. Sharma, R. Flores-Moreno, K. Mohanty, and S.A. Hariprasad, Sci. Rep. 12 (2022) 20292.

- [13] Y. Kitamura, N. Okinaka, T. Shibayama, O.O.P. Mahaney, D. Kusano, B. Ohtani, and T. Akiyama, *Powder Technol.* 176 (2007).
- [14] R.S. Bhat, and A.C. Hegde, *Anal. Bioanal. Electrochem.* 16 (2024) 258.
- [15] R.S. Bhat, M.K. Balakrishna, P. Parthasarathy, and A.C. Hegde, *Coatings* 13 (2023) 772.
- [16] R.S. Bhat, and A.G. Bindu, *J. Environ. Chem. Eng.* 11 (2025) 116046.
- [17] A.J.S. Ahammad, S. Sarker, M.A. Rahman, and J.J. Lee, *Electroanalysis* 22 (2010) 694.
- [18] X.B. Zhou, Z.F. He, Q.W. Lian, Z. Li, H. Jiang, and X.Q. Lu, *Sens. Actuators B* 193 (2014) 198.
- [19] F.X. Hu, S.H. Chen, C.Y. Wang, R. Yuan, D.H. Yuan, and C. Wang, *Anal. Chim. Acta* 724 (2012) 40.
- [20] Z.C. Meng, H.F. Zhang, and J.B. Zheng, *Res. Chem. Intermed.* 39 (2013) 3135.